JOURNAL OF AIRCRAFT
Vol. 45, No. 2, March–April 2008

Engineering Notes

ENGINEERING NOTES are short manuscripts describing new developments or important results of a preliminary nature. These Notes should not exceed 2500 words (where a figure or table counts as 200 words). Following informal review by the Editors, they may be published within a few months of the date of receipt. Style requirements are the same as for regular contributions (see inside back cover).

Effect of the Blade Inner-Tip Position on the Generation of Twin Vortices

Jiyoung Jung,* Wooyoung Choi,† and Soogab Lee‡
Seoul National University, Seoul 151-742, Republic of Korea

DOI: 10.2514/1.34549

Nomenclature

C_P	=	pressure coefficient
C_Q	=	torque coefficient
C_q	=	sectional torque coefficient
C_T	=	thrust coefficient
C_t	=	sectional thrust coefficient
$\hat{\boldsymbol{F}}_I, \hat{\boldsymbol{G}}_I, \hat{\boldsymbol{H}}_I$	=	inviscid fluxes in the ξ, η, and ζ directions
$\hat{\boldsymbol{F}}_V, \hat{\boldsymbol{G}}_V, \hat{\boldsymbol{H}}_V$	=	viscous fluxes in the ξ, η, and ζ directions
J	=	Jacobian of transformation
$\boldsymbol{q}$	=	conserved variable vector
u, v	=	velocity components in the x and y directions
ξ, η, ζ	=	computational domain coordinates
ρ	=	air density
σ	=	rotor solidity
τ	=	nondimensional time
Ω	=	rotational speed

I. Introduction

BLADE–VORTEX interaction (BVI) is one of the major noise sources in helicopters that occurs when the helicopter blades collide or come close to the vortices from previous blades in descent flight [1]. Many studies have been conducted to alleviate this undesirable phenomenon by modifying blade tip shape. One of the concepts is to generate twin tip vortices. Some studies have examined the generation of twin tip vortices and the interaction between the vortices and following blades.

Beddoes and Pike [2] proposed the concept of twin vortices as a strategy to BVI reduction through the theoretical research about the idealized blade–vortex interaction of twin vortices. It was shown that the amplitude of BVI is reduced, whereas the waveform remains the same as that of single vortex interaction, if the distance between vortices is shorter than one chord length. This study showed that the impulsive loading could be relived by splitting the vortex into two smaller equal-strength vortices.

After that, a few blades have been designed based on that concept, and the vane-tip blade is one of them. The design process and the test results of a vane-tip blade were reported by Brocklehurst and Pike [3]. The vane-tip blade was initially designed by an analytical approach, which could generate twin tip vortices with minimal performance penalty. In the wind-tunnel test, the twin tip vortices were generated by the vane-tip blade and a significant reduction in BVI was achieved.

There is another type of blade generating twin tip vortices that was proposed and numerically tested by Hwang et al. [4]. It was entitled the Korean BERP (British Experimental Rotor Program) blade (KBERP) and was designed by combining the twin-vortex-generation concept and the BERP blade concept. In the study, the effects of several parameters were numerically investigated. The parameters are related to separation distance, circulation portion, and core radii of the tip vortices. It was also reported that KBERP could reduce BVI noise.

The shapes of the blades are quite different from each other, but they have an inner-tip structure in common, which generates the inner-tip vortex. The inner tip is formed by reducing the chord length abruptly near the tip region. The position of the inner tip can be selected at the fore or aft of the blade in the chordwise direction; examples are the KBERP blade and vane-tip blade, respectively (Fig. 1).

These previous studies were mainly focused on the blade shape to generate twin tip vortices. On the other hand, there were several experimental studies that focused not on the generation of a twin-vortex system, but on the characteristics of the twin tip vortices themselves. In these studies, twin tip vortices were generated by combining conventional wing-vortex generators.

The flowfield of corotating twin tip vortices was investigated by Copland et al. [5] at the wind tunnel of the University of Glasgow using two wing-vortex generators. It was shown that the core size of the twin tip vortices grew almost linearly with downstream distance and that the distance between the vortices remains almost constant. The test results of the vortex trajectory were compared with the solution of the simple vortex core model and they showed good agreement.

Recently, Coton et al. [6] performed an experimental study about the interaction of twin tip vortices and a rotating blade in a wind tunnel. The twin tip vortices were generated by two wing-vortex generators and a nonlifting rotating rotor was mounted downstream of the vortex generators. This experimental study showed that the fluctuation of blade surface pressures is sensitive to the inclination angle of vortices relative to the blade and the separation distance of the vortex pair.

Until relatively recently, few studies were done on the effect of tip-shape parameters on the generation of twin tip vortices. The concept of twin tip vortices could be combined with established blades, as shown in [4]. The blade tip region is closely related to the aerodynamic performance. As a consequence, the tip region should be carefully treated when the concept is combined. It is important to understand the characteristics of twin tip vortices as variation of parameters. Two tip structures are necessary to generate twin tip vortices, and the distribution of tip positions should be determined. In the radial position, one tip is placed at the end of the blade and the other is placed a little inboard from the end of the blade. The distance between the vortices is greatly related to the radial distribution of tips that would be adjusted properly. The inner tip, in the aspect of

Received 12 September 2007; revision received 5 October 2007; accepted for publication 5 October 2007.

*Ph.D. Candidate, School of Mechanical and Aerospace Engineering; nicejjy1@snu.ac.kr.

†Ph.D. Candidate, School of Mechanical and Aerospace Engineering; yanni1@snu.ac.kr.

‡Professor, School of Mechanical and Aerospace Engineering; solee@snu.ac.kr. Member AIAA.

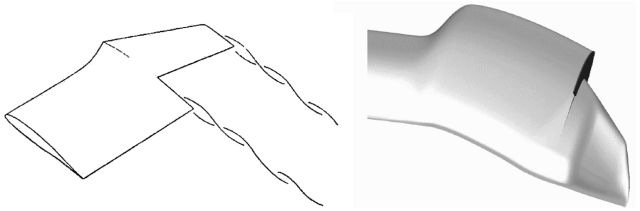

a) Vane tip blade b) KBERP blade

Fig. 1 Tip shapes of the vane-tip blade and KBERP blade.

chordwise position, could be started from the leading edge and ended at the middle of the blade or could be started from the middle of the blade and ended at the trailing edge. The chordwise positions of the tips are greatly related to the formation of the vortex, which is a matter of choice that should be precede the modulation of radial position and tip length in adopting the twin-vortex-generation concept.

This study examines the effect of chordwise position of the inner tip on the rotor performance and generation of twin tip vortices in hover. Two blades generating twin tip vortices were conceptually designed for this study. Flowfields of three rotor blades were numerically analyzed in hover. For that, a three-dimensional Navier–Stokes equations solver was used; the solver named HeliNA was combined with the fifth order of weighted essentially nonoscillatory (WENO) [7,8] scheme and overset grids to capture the vortex accurately. The performance results of the blades were compared with each other. The formation and structure of vortices were analyzed. These results give a suggestion on the choice of the inner-tip position in adopting the twin-vortex-generation concept.

II. Numerical Method: HeliNA

Helicopter Navier–Stokes equations solver HeliNA was used for flowfield analysis. The solver was developed at the Aeroacoustics and Noise Control Laboratory in Seoul National University and was based on the three-dimensional Reynolds-averaged Navier–Stokes equations. Roe's flux difference splitting scheme combined with the fifth order of WENO approach [7,8] was applied for higher-order spatial accuracy. The lower–upper symmetric Gauss–Seidel method was used for the time integration. Turbulent viscosity was considered using the Baldwin–Lomax turbulence model [9].

To reduce the computational load, the source-term formulation proposed by Chen et al. [10] was implemented as the governing equation instead of the moving-grid technique [Eqs. (1) and (2)]:

$$\frac{\partial q}{\partial \tau} + \frac{\partial \hat{\boldsymbol{F}}_I}{\partial \xi} + \frac{\partial \hat{\boldsymbol{G}}_I}{\partial \eta} + \frac{\partial \hat{\boldsymbol{H}}_I}{\partial \zeta} = \frac{\partial \hat{\boldsymbol{F}}_V}{\partial \xi} + \frac{\partial \hat{\boldsymbol{G}}_V}{\partial \eta} + \frac{\partial \hat{\boldsymbol{H}}_V}{\partial \zeta} + R \qquad (1)$$

$$R = J^{-1}(0 \;\; \Omega\rho v \;\; -\Omega\rho u \;\; 0 \;\; 0)^T \qquad (2)$$

The computational domain was constructed around one blade for efficient computation, and periodic boundary condition was applied. For the far boundaries, the source-sink model was adopted to prescribe the rotor outflow below the blade by the 1-D momentum theory that was proposed by Srinivasan et al. [11].

To capture the tip vortex with high accuracy, the overset grid technique was used. The grid system was composed of five grids: one C-H type of main grid around the rotor, three H-H type grids to capture the vortices accurately, and one H-H type of background grid (Fig. 2). Two-cell overlaps were used between the main grid and the subgrid. The C-H grid on the rotor contains $161 \times 110 \times 50$ grids point in the chordwise, spanwise, and normal directions. The H-H grid on the tip-vortex region contains $110 \times 150 \times 50$ grids point in the radial direction, normal direction, and azimuthal direction. The total grid point was about 4.5 million. The code was calculated on a PC parallel machine.

III. Blades and Calculation Condition

Three types of blades were used for hovering calculations, and the tip shapes are shown in Fig. 3. One is the baseline blade generating a general single tip vortex and others are designed to generate twin tip vortices. For the baseline, a rectangular and untwisted blade with a 15.5 aspect ratio was used. The aspect ratio was adopted from the UH-60A validation case. Started from the baseline blade, two blades were designed to generate twin tip vortices. In this study, the inner tip was designed by only modifying the chord length near the tip region. Other shape parameters were excluded to focus on the position of the inner tip. The first blade for generating twin tip vortices was designed by placing the inner tip of 0.5 chord length at the leading edge. The second blade was designed through a process similar to first one, except that the inner tip was started from the middle of the blade in the chordwise direction and ended at the trailing edge. The blades were named the leading-tip blade and trailing-tip blade, based on the position of the inner tip, for convenience. The spanwise position of the inner tip was set as 96% of the radius (60% chord inboard from the outer tip of the blade). The radial position was chosen from a simple study that the blades could generate separated twin tip vortices. For the sectional airfoil, NACA0012 was used. All cases were calculated in a four-bladed rotor condition, and the tip Mach number was 0.628.

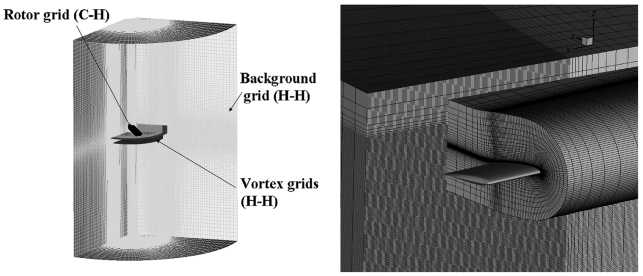

Fig. 2 Grid system.

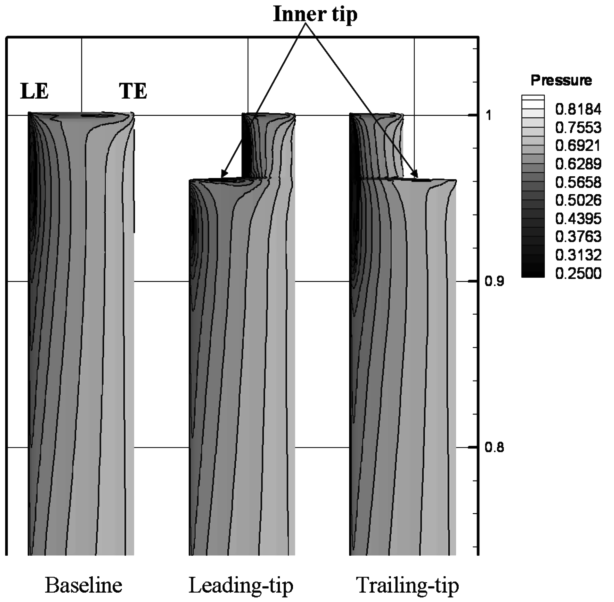

Fig. 3 Blade tip shapes and pressure contours in a collective pitch of 8 deg.

IV. Hovering Results

A. Validation Case

The hovering calculation result was validated by comparing with the UH-60A helicopter experimental data, which were tested by Lorber et al. [12]. The computed torque coefficient variation as a thrust condition is shown in Fig. 4. The prediction results showed good agreement with the experimental data. For a more detailed comparison, pressure distributions at several radial positions are presented in Fig. 5.

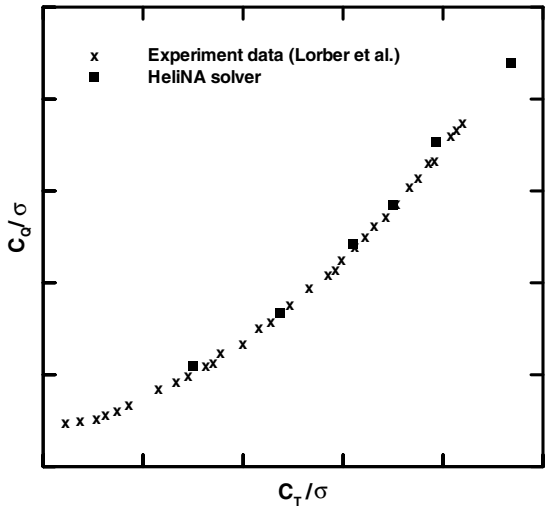

Fig. 4 Torque versus thrust of the UH-60A blade in hover.

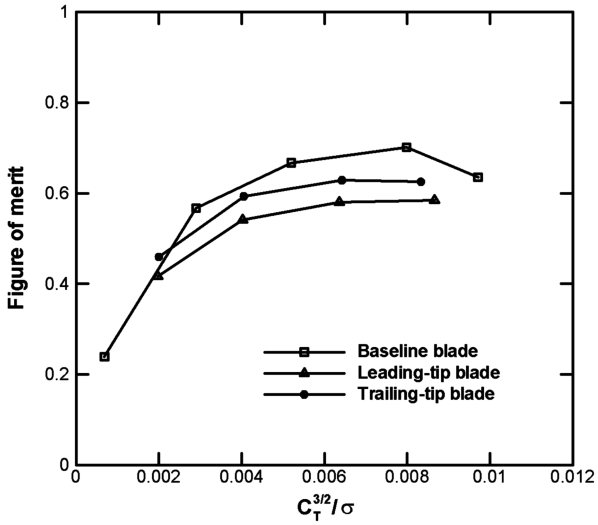

Fig. 6 Figure of merit versus thrust variation.

B. Performance of Rotor Blades in Hover

The calculation results of hover performance are shown in Fig. 6 in terms of the figure of merit. The performance of the two blades generating twin tip vortices almost agreed with that of the baseline blade in the low thrust. However, the difference of performance grew as the thrust increased. The trailing-tip blade showed slightly higher performance than the leading-tip blade through all of the thrust range. We found that the performance difference between the twin-vortex-generating blades are mainly because of the torque difference. This will be explained with Fig. 7.

Figure 7a shows the sectional thrust of the three blades at the collective pitch of 8 deg. After the inner-tip position ($r/R = 0.96$), the thrust was dropped abruptly in cases of the blades generating twin tip vortices. The loss of sectional thrust was more severe in the leading-tip blade at the region from $r/R = 0.96$ to 0.98. However, the leading-tip blade showed a narrow high peak just inboard of the inner tip. At the region from $r/R = 0.9$ to 0.94, the two blades showed a higher thrust value than the baseline blade. It can be seen that the thrust peak appears more inboard compared with the baseline blade, and this is because the vortex generated the previous blade pass more inboard than the baseline (Figs. 8a–8c). In Fig. 8, the tip-vortex position of the baseline is indicated with a vertical dotted line.

The sectional torque is shown as the radial position in Fig. 7b. It is interesting that a peak always appears just before the tips in all blades. In the case of the leading-tip blade, the peak of the inner tip was much higher than that of the trailing-tip blade, even compared with the baseline. Though the sectional torque of the leading-tip blade showed the lowest value from 96% of the radius to the outer tip, the integrated torque value was higher than that of the trailing-tip blade. This mainly causes the performance loss shown in Fig. 6. The torque of the trailing-tip blade also had two peaks at the tips. However, the magnitude of each peak was much lower than those of other blades.

The inner tip of the leading-tip blade was placed at the fore half of the chord, where most of the lift is produced. Thus, the upward flow from the pressure side to the suction side was stronger in the leading-tip blade than in the trailing-tip blade. As a consequence, the formation of the inner vortex affected the performance more in the leading-tip blade. The narrow peak, shown in the sectional thrust of the leading-tip blade, could be explained by the effect of the inner vortex flown over the rear part of the upper surface in the leading-tip blade. In the leading-tip-blade case, the unusual high peak of sectional torque comes from the effect of strong upwash caused in the roll-up process and the previous vortex passage. As shown in Fig. 8b, the inner tip of the leading-tip blade is the nearest to the previous vortex, compared with other blades, and this may causes the high magnitude of sectional torque. Based on the results, it could be deduced that the performance of the trailing-tip blade has strong points compared with the leading-tip blade, if the chordwise length and radial position of the inner tip are the same.

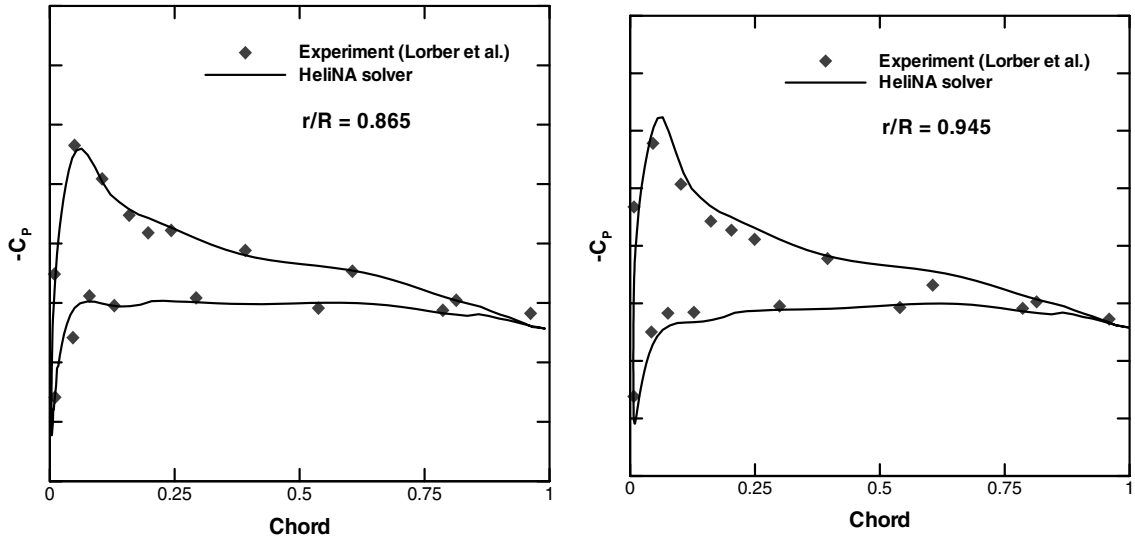

a) r/R=0.865 b) r/R=0.945

Fig. 5 Sectional pressure distribution of the UH-60A rotor in hover.

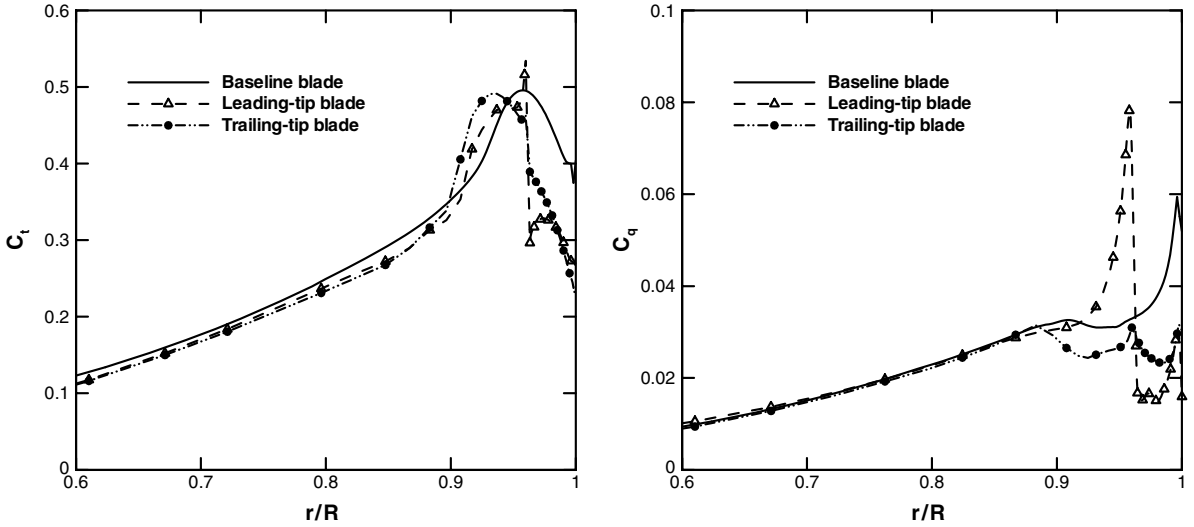

a) Sectional thrust b) Sectional torque

Fig. 7 Sectional thrust and torque in a collective pitch of 8 deg.

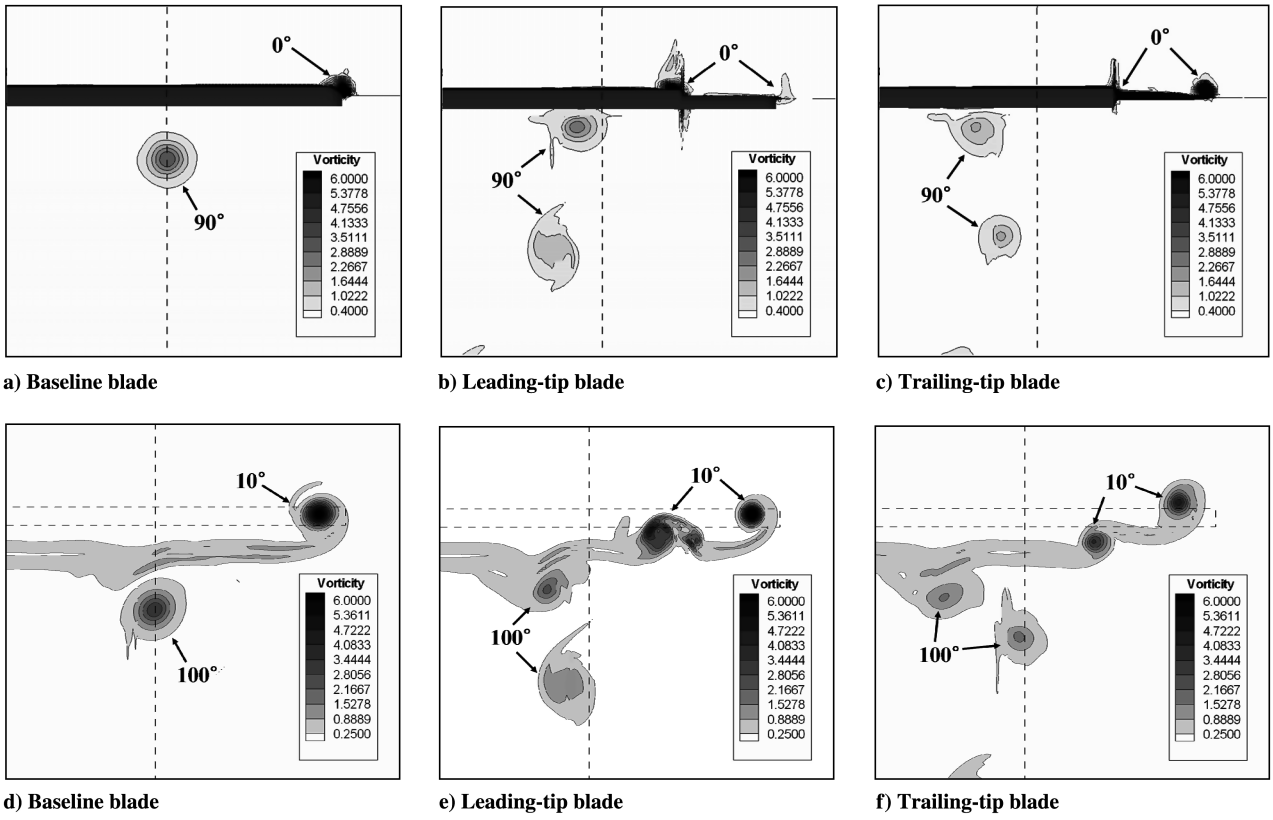

a) Baseline blade b) Leading-tip blade c) Trailing-tip blade

d) Baseline blade e) Leading-tip blade f) Trailing-tip blade

Fig. 8 Vorticity contours of hovering rotors in azimuthal positions of a–c) 0 deg and d–f) 10 deg.

C. Vortex Structure

The vortex structures were analyzed because it is important in the twin-vortex-generation concept to distribute the circulation into two tip vortices evenly. In Fig. 8, the vorticity contours of three blades are shown at the plane of 0- and 10-deg azimuthal positions. Separated twin tip vortices are clearly shown in both cases. The vorticity is highest in the center of the vortex, and the contour forms concentric circles in the conventional tip vortex. Most vortices showed the conventional feature of vorticity in the figure at an azimuth of 10 deg. However, in the inner vortex of the leading-tip blade, two vortical structures were observed. The vorticity of the inboard larger vortical structure was widely distributed, and the maximum point appeared slightly inboard and upward from the vortex center. The schematic sketch is shown in Fig. 9 of the roll-up of the inner vortex in the leading-tip blade. The upwash flow formed at the inner tip is blocked by the rear part of the blade. It is shown how the two vortical structures appeared and how they disturb the surface near the inner-tip region. The unusual peak shown in Fig. 7b might be caused by this disturbance. It was observed (not shown here) that the roll-up process takes longer to complete in the inner vortex of the leading-tip blade.

The result of vortex circulation is shown in Fig. 10 as thrust variation. The azimuthal position was determined as 30 deg by considering the completion of the roll-up process. The circulation was calculated from the core radius, and the maximum tangential velocity of the vortices was extracted from the computational result. The total circulation of tip vortices in twin-vortex-generating blades

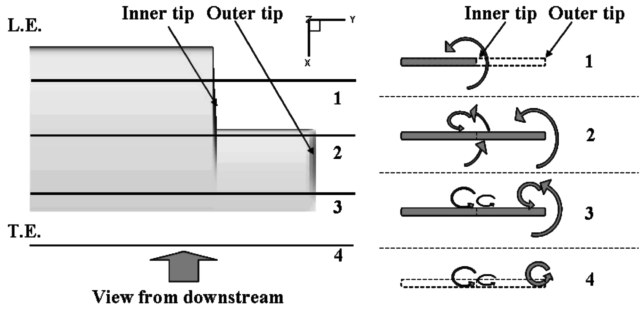

Fig. 9 Schematic sketch about the vortex formation in the leading-tip blade.

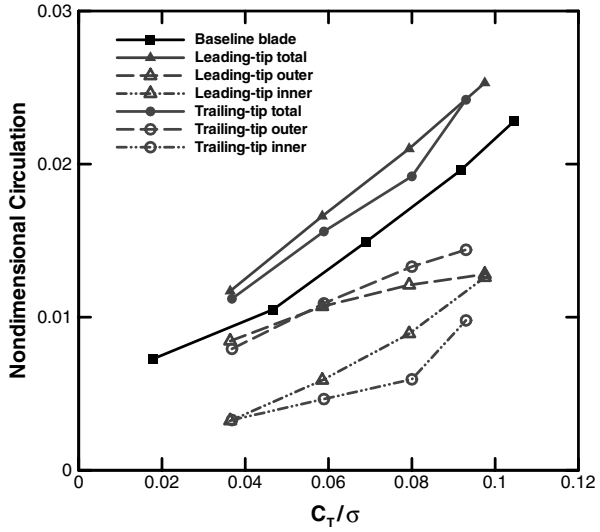

Fig. 10 Nondimensional circulation of vortices at an azimuthal plane of 30 deg.

was linearly increased as thrust increased. As the thrust increased, the difference between the inner- and outer-tip vortices was increased in the trailing-tip-blade case. In the leading-tip-blade case, however, the difference was decreased as thrust increased and tip vortices with the same circulation were generated near $C_T/\sigma = 0.1$. This can be also explained with the position of the inner tip. The circulation of vortices is related to the pressure differences of the upper and lower surfaces near the tip. As the thrust is increased, the pressure difference of the surfaces near the tip is increased and the rate of increment is higher in the leading-tip blade. Moreover, as the inner vortex becomes stronger, the effect of upwash flow is increased, which causes the loss of thrust outside of the inner tip. This might cause a slower increase of outer vortex circulation compared with trailing-tip-blade case.

In the concept of a twin-vortex-generating blade, it is important to generate two tip vortices of the same strength at least 0.5 chord apart with minimal performance degradation [2]. It was observed that both twin-vortex-generating blades could generate separated tip vortices in various thrust conditions. Though two blades could generate twin tip vortices, the trailing-tip blade showed an advantage in the aspect of performance, and so it seems to be the choice.

V. Conclusions

The effect of the chordwise inner-tip position was examined with conceptually designed blades that generate twin tip vortices. The three-dimensional Navier–Stokes solver HeliNA was used for flowfield analysis. The solver was combined with overset grids and validated by comparing with the experimental data of the UH-60A rotor. Two blades were designed by reducing the chord length by a half-chord near the tip region.

The trailing-tip blade showed higher performance and it was due to the lower sectional torque near the inner tip. Both blades generated a separated twin-vortex structure. The inner vortex of the trailing-tip blade was generated in a similar way to the conventional tip vortex, but that of the leading-tip blade was formed with a more distributed vorticity structure. The strength of the inner-tip vortex was weaker than the outer-tip vortex in hover. The difference of circulation between the inner and outer vortices was increased in the trailing-tip blade and was decreased in the leading-tip blade as thrust increased.

With the same length of the inner tip at the same radial position, the trailing-tip blade showed an advantage compared with the leading-tip blade in the aspect of performance. It was indicated that the differences mainly come from the pressure difference between the upper and lower sides inboard of the inner tip. Moreover, the inner vortex of the leading-tip blade disturbs the flow on the rear of the blade surface. The results might provide an intuition for choosing the position of the inner tip in the blade design process of adopting the twin-vortex generation concept.

Acknowledgments

This study was supported by the Korea Aerospace Research Institute (KARI) under the Korean Helicopter Program (KHP) Dual-Use Component Development Program funded by the Ministry of Commerce, Industry and Energy (MOCIE). This work is the outcome of the fostering project of the Best Lab, supported financially by the MOCIE.

References

[1] Yu, Y. H., "Rotor Blade–Vortex Interaction Noise," *Progress in Aerospace Sciences*, Vol. 36, No. 2, Feb. 2000, pp. 97–115. doi:10.1016/S0376-0421(99)00012-3

[2] Beddoes, T. S., and Pike, A. C., "Noise Reduction with a Twin Tip Vortex Configuration," *52nd AHS International Forum*, AHS International, Alexandria, VA, June 1996, pp. 45–58.

[3] Brocklehurst, A., and Pike, A. C., "Reduction of BVI Noise Using a Vane Tip," *AHS Aeromechanics Specialists Conference*, AHS International, Alexandria, VA, 19–21 Jan. 1994.

[4] Hwang, C., Joo, G., Pike, A. C., and Perry, F. J., "Parametric Study for the Low BVI Noise BERP Blade: KBERP Design Using DEAF," *27th European Rotorcraft Forum* [CD-ROM], Royal Aeronautical Society, London, 11–14 Sept. 2001, pp. 13.1–13.9.

[5] Copland, C. M., Coton, F. N., and Galbraith, R. A. McD., "An Experimental Study of the Idealized Vortex System of a Novel Rotor Blade Tip," *The Aeronautical Journal*, Vol. 102, No. 1017, Aug.—Sept. 1998, pp. 385–392.

[6] Coton, F. N., Green, R. B., and Galbraith, R. A. McD., "Analysis of Model Rotor Blade Pressures During Parallel Interaction with Twin Vortices," *Journal of Aircraft*, Vol. 42, No. 6, Nov.–Dec. 2005, pp. 1553–1565.

[7] Jiang, G.-S., and Shu, C.-W., "Efficient Implementation of Weighted ENO Schemes," *Journal of Computational Physics*, Vol. 126, No. 1, 1996, pp. 202–228. doi:10.1006/jcph.1996.0130

[8] Usta, E., Wake, B. E., Egolf, T. A., and Sankar, L. N., "Application of a Symmetric Total Variation Diminishing Scheme to Aerodynamics and Aeroacoustics of Rotors," *57th Annual Forum of American Helicopter Society* [CD-ROM], AHS International, Alexandria, VA, 9–11 May 2001.

[9] Baldwin, B. S., and Lomax, H., "Thin Layer Approximation and Algebraic Model for Separated Turbulent Flow," AIAA Paper 78-257, 1978.

[10] Chen, C. L., McCroskey, W. J., and Obayashi, S., "Numerical Solutions of Forward-Flight Rotor Flows Using an Upwind Method," *Journal of Aircraft*, Vol. 28, No. 6, 1991, pp. 374–380.

[11] Srinivasan, G. R., Raghavan, V., Duque, E. P. N., and McCroskey, W. J., "Flow Field Analysis of Modern Helicopter Rotors in Hover by Navier–Stokes Method," *Journal of the American Helicopter Society*, Vol. 38, No. 3, 1993, pp. 1–11.

[12] Lorber, P. F., Stauter, R. C., and Landgrebe, A. J., "A Comprehensive Hover Test of the Airloads and Airflow of an Extensively Instrumented Model Helicopter Rotor," *45th Annual Forum of American Helicopter Society*, AHS International, Alexandria, VA, May 1989, pp. 281–295.